Check for updates

LIMNOLOGY and OCEANOGRAPHY

ASLO

Limnol. Oceanogr. 63, 2018, 2140–2153
© 2018 Association for the Sciences of Limnology and Oceanography
doi: 10.1002/lno.10929

Recovery of Holothuroidea population density, community composition, and respiration activity after a deep-sea disturbance experiment

Tanja Stratmann,[1]* Ilja Voorsmit,[2] Andrey Gebruk,[3] Alastair Brown,[4] Autun Purser,[5] Yann Marcon,[5,6] Andrew K. Sweetman,[7] Daniel O. B. Jones,[8] Dick van Oevelen[1]

[1]NIOZ Royal Netherlands Institute for Sea Research, Department of Estuarine and Delta Systems, and Utrecht University, Yerseke, The Netherlands
[2]Faculty of Mathematics and Natural Sciences, University of Groningen, Groningen, The Netherlands
[3]P.P. Shirshov Institute of Oceanology, Russian Academy of Sciences, Moscow, Russia
[4]Ocean and Earth Science, University of Southampton, National Oceanography Centre Southampton, Southampton, United Kingdom
[5]Deep Sea Ecology and Technology, Alfred Wegener Institute, Bremerhaven, Germany
[6]MARUM, Center for Marine Environmental Sciences, Bremen, Germany
[7]The Marine Benthic Ecology, Biogeochemistry and In-Situ Technology Research Group, The Lyell Centre for Earth and Marine Science and Technology, Heriot-Watt University, Edinburgh, United Kingdom
[8]Ocean Biogeochemistry and Ecosystems, National Oceanography Centre Southampton, Southampton, United Kingdom

Abstract

Mining polymetallic nodules on abyssal plains will have adverse impacts on deep-sea ecosystems, but it is largely unknown whether the impacted ecosystem will recover, and if so at what rate. In 1989 the "DISturbance and reCOLonization" (DISCOL) experiment was conducted in the Peru Basin where the seafloor was disturbed with a plough harrow construction to explore the effect of small-scale sediment disturbance from deep-sea mining. Densities of Holothuroidea in the region were last investigated 7 yr post-disturbance, before 19 yr later, the DISCOL site was re-visited in 2015. An "ocean floor observatory system" was used to photograph the seabed across ploughed and unploughed seafloor and at reference sites. The images were analyzed to determine the Holothuroidea population density and community composition, which were combined with in situ respiration measurements of individual Holothuroidea to generate a respiration budget of the study area. For the first time since the experimental disturbance, similar Holothuroidea densities were observed at the DISCOL site and at reference sites. The Holothuroidea assemblage was dominated by *Amperima* sp., *Mesothuria* sp., and *Benthodytes typica*, together contributing 46% to the Holothuroidea population density. Biomass and respiration were similar among sites, with a Holothuroidea community respiration of $5.84 \times 10^{-4} \pm 8.74 \times 10^{-5}$ mmol C m^{-2} d^{-1} at reference sites. Although these results indicate recovery of Holothuroidea, extrapolations regarding recovery from deep-sea mining activities must be made with caution: results presented here are based on a relatively small-scale disturbance experiment as compared to industrial-scale nodule mining, and also only represent one taxonomic class of the megafauna.

Interest in mining polymetallic nodules from abyssal plains has increased substantially since the 1960s (Glasby 2000; Jones et al. 2017). Polymetallic nodules contain valuable metals such as copper, cobalt, nickel, and rare earth elements (Wang and Müller 2009) and are therefore considered economically interesting resources. However, deep-sea mining activities will have negative impacts on these vulnerable deep-sea ecosystems through the removal of hard substratum (i.e., polymetallic nodules) essential for sessile (e.g., Amon et al. 2016; Vanreusel et al. 2016) and mobile (Leitner et al. 2017; Purser et al. 2016) fauna. Further negative impacts may result from the disturbance and/or removal of the upper sediment layer (Thiel and Tiefsee-Umweltschutz 2001), i.e., the habitat that contains the majority of organisms and their food sources (Danovaro et al. 1993, 1995;

*Correspondence: tanja.stratmann@nioz.nl

Haeckel et al. 2001). Sessile fauna and infauna will be removed in the mining tracks (Borowski and Thiel 1998; Bluhm 2001; Borowski 2001), and fauna in and on adjacent sediments may be blanketed by mechanically displaced sediment (Thiel and Tiefsee-Umweltschutz 2001). Re-suspended sediment and sediment plumes may smother both sessile and mobile fauna over extended areas, or potentially adversely impact filter feeding organisms (Jankowski and Zielke 2001; Thiel and Tiefsee-Umweltschutz 2001; Brooke et al. 2009).

Ecological concerns about deep-sea mining have resulted in several deep-sea experiments studying ecosystem recovery following disturbance (Jones et al. 2017). To investigate the recovery from small scale disturbance experiments employing isolated individual disturbance tracks, Vanreusel et al. (2016) used ROV video surveys to compare sessile and mobile metazoan epifauna densities at disturbed and undisturbed sites with high and low "polymetallic nodule" coverage in the Clarion-Clipperton Zone (CCZ, central Pacific). The mobile metazoan epifauna in a 20-yr-old experimental mining track at a nodule-free site comprised mainly Holothuroidea and Ophiuroidea (1500 ind. ha^{-1}), whereas the density at the reference site was substantially higher (3000 ind. ha^{-1}). In contrast, the same study showed that mobile metazoan epifauna at a nodule-rich site in another, 37-yr-old mining track in the CCZ consisted exclusively of Echinoidea (1000 ind. ha^{-1}) and had a 70% lower mobile epifauna density than the reference site, where Holothuroidea and Ophiuroidea were also present.

The most extensively studied and largest-scale disturbance experiment conducted to date is the "DISturbance and reCOLonization experiment" (DISCOL) in the Peru Basin. This experiment was conducted in a 10.8 km^2 circular area, DISCOL Disturbance Area or "DEA" in short, which was ploughed 78 times on diametric courses in 1989 to mimic a small-scale deep-sea mining disturbance event (Foell et al. 1990, 1992; Bluhm 2001). The DEA can be considered "small-scale" in comparison to commercial mining as the 10.8 km^2 represent between 1.4% and 3.6% of the area projected to be disturbed by one individual mining operation per year (Smith et al. 2008). The imposed disturbance occurred on two levels: (1) direct impacts inside "plough tracks" where polymetallic nodules were ploughed into the sediment ($\sim$ 22% of DEA) and (2) indirect impacts from plume exposure associated with the ploughing outside plough tracks ($\sim$ 70–75% of the DEA; Thiel and Schriever 1989; Bluhm and Thiel 1996). Four sites, each approximately 4 km away from the DEA served as reference areas as they were considered to be outside the area of plume influence.

Biological investigations were conducted inside the disturbance tracks, outside the tracks and at the reference sites prior to the DISCOL disturbance (reference sites; DISCOL 1/1 cruise), immediately following DISCOL disturbance (inside and outside tracks; DISCOL 1/2 cruise) and half a year (DISCOL 2 cruise), three (DISCOL 3 cruise), and 7 yr (ECOBENT cruise) post DISCOL disturbance (Bluhm 2001) to assess ecosystem recovery over time. The disturbance experiment impacted the meiofaunal, macrofaunal, and megafaunal size classes of the benthic community, but the magnitude of disturbance differed markedly among size classes and functional groups. For example, the abundance of meiofaunal harpacticoids was approximately 20% lower at the disturbed sites compared to the undisturbed sites immediately following the DISCOL disturbance, a difference that persisted up to 7 yr after the DISCOL disturbance (Ahnert and Schriever 2001). In contrast, total macrofauna abundance at the disturbed sites was 66% lower than at the undisturbed sites immediately following the DISCOL disturbance, but was similar between disturbed and undisturbed sites 3 yr after the DISCOL disturbance (Borowski 2001). Sessile megafauna, such as Cnidaria, Crinoidea, and Ascidiacea, was virtually absent from disturbed sites following ploughing, and did not recover to pre-disturbance densities during the subsequent 7 yr (Bluhm 2001). Their slow recovery is likely a result of the removal of hard substratum from the seafloor (Vanreusel et al. 2016). Total megafaunal densities were significantly lower in the disturbed sites directly after the DISCOL disturbance, half a year after and 7 yr after the DISCOL disturbance, but not significantly different 3 yr after the DISCOL disturbance (Bluhm 2001). Holothuroidea, the dominant taxa of mobile megafauna, remained reduced at disturbed sites (75 ± 50 ind. ha^{-1}) when compared with densities observed at undisturbed sites (169 ± 79 ind. ha^{-1}) 7 yr after the DISCOL disturbance (Bluhm 2001), though the difference was not statistically significant because of the large variability within the data.

These deposit-feeding Holothuroidea are a key component of abyssal benthic communities as they engage in key ecosystem functions of the deep sea, such as modifying the quality of the organic matter of the sediment (Smallwood et al. 1999), processing of fresh phytodetritus (Bett et al. 2001; FitzGeorge-Balfour et al. 2010), and mineralization through nutrient regeneration or respiration (Thurber et al. 2014). Holothurians make a contribution to mineralization as they were estimated to respire between 1% and 6% of the particulate organic carbon flux per year on Pacific and Atlantic abyssal plains (Ruhl et al. 2014). Many holothurian species are large in comparison to other abyssal benthic invertebrates and can therefore be counted and identified from images with comparative ease (Durden et al. 2016). Holothuroidea are also mobile, with some species moving > 100 cm h^{-1} over the seafloor (Jamieson et al. 2011) and some species having the capacity to swim (Miller and Pawson 1990; Rogacheva et al. 2012). Holothuroidea can respond to fresh phytodetritus deposition events with large-scale recruitment within a year (Billett et al. 2010). One would therefore expect that Holothuroidea may recover in regions of disturbed seafloor comparatively quickly.

19395590, 2018, 5, Downloaded from https://aslopubs.onlinelibrary.wiley.com/doi/10.1002/lno.10929 by University Of Chemistry And, Wiley Online Library on [01/10/2026]. See the Terms and Conditions (https://onlinelibrary.wiley.com/terms-and-conditions) on Wiley Online Library for rules of use; OA articles are governed by the applicable Creative Commons License

In this study, we assessed Holothuroidea population density and community composition 26 yr after the initial disturbance at the DISCOL area, by determining abundances from high-resolution photos taken of the seafloor both within and outside plough tracks, and at reference sites south and southeast of the DEA. The results of this abundance estimation were then combined with in situ respiration rate measurements to identify any differences in respiratory activity of Holothuroidea at the various sites. These data were compared with earlier Holothuroidea population density data to investigate (1) whether the Holothuroidea assemblages differed between disturbed, undisturbed and reference areas, (2) whether Holothuroidea population densities had recovered after 26 yr, and (3) whether Holothuroidea respiration rates differed between sites. The mechanisms underlying the observed recovery dynamics are discussed and considered in the context of future mining operations.

Methods

Study site

The seafloor in the Peru Basin in the tropical south-east Pacific Ocean is typically between 4000 m and 4400 m deep (Wiedicke and Weber 1996), has a bottom water temperature of 2.9°C, salinity of 34.6 PSU, and oxygen concentration of 145.3 ± 1.3 (mean ± SD) μmol L^{-1} (Boetius 2015). Bottom water currents alternate between periods of comparatively strong (> 5 cm s^{-1}) unidirectional currents and periods of slower (< 1–3 cm s^{-1}) current flow without prevalent direction (Klein et al. 1975). The DEA itself is centered on 07°04.4′S, 88°27.6′W and is between 4140 m and 4160 m deep (Bluhm et al. 1995). Sediment in the DEA typically consists of a 5–15 cm thick surface layer of semi-liquid, dark brown sediment (0.55% ± 0.11% organic carbon) and a sub-layer of consolidated greyish clay (0.70% ± 0.08% organic carbon) (Grupe et al. 2001; Marchig et al. 2001; Oebius et al. 2001). Surface sediments in the DEA have 18.1 ± 11.3 kg m^{-2} of polymetallic nodules (Marchig et al. 2001). The DEA plough tracks are still clearly visible (Fig. 1) and consequently we identified three disturbance categories for the study: inside and outside plough tracks in the DEA (hereafter referred to as disturbed site and undisturbed site respectively), and reference sites south and southeast of the DEA (hereafter referred to as reference site) (Fig. 1).

Assessment of holothuroidea assemblage

A high-resolution digital camera (CANON EOS 5D Mark III, modified for underwater applications by iSiTEC) on the towed Ocean Floor Observation System (OFOS) was used to photograph the seafloor. The OFOS was deployed from the RV *Sonne* during cruise SO242-2 (chief scientist: Prof. Dr. Antje Boetius) and towed 1.5 m above the seafloor at a speed of approximately 0.5 knots, photographing the seafloor every 10 s (~ 5.5 m^2 seafloor per image) (Purser et al. 2016). In contrast, during previous DISCOL cruises (from directly following to 7 yr after the DISCOL disturbance), the OFOS was equipped with analog still-photo cameras (DISCOL 1/1, DISCOL 1/2 and DISCOL 2 cruises: Benthos 377 camera; DISCOL 3 and ECOBENT cruises: Photosea 5000 camera; Bluhm et al. 1995; Schriever et al. 1996). For these deployments, the system was towed approximately 3 m above the seafloor and the photographs were taken selectively by scientists (Bluhm and Gebruk 1999; Jones et al. 2017).

For this study, the OFOS was deployed four times at the DEA (Fig. 1; Table 1), where a total of 3760 usable (neither under- nor overexposed, correct altitude and without suspended sediment obscuration) pictures were taken. Images were classified as "disturbed site" when plough tracks were visible (1838 photos) and otherwise classified as "undisturbed site" (1922 photos; Table 1). The OFOS was also deployed four times for this study at reference sites outside the DEA (Fig. 1; Table 1), where a total of 983 usable pictures were taken. Each transect was treated as a replicate resulting in four replicates for each level of disturbance (i.e., disturbed, undisturbed, and reference site).

Photographs were loaded into the open-source software "Program for Annotation of Photographs and Rapid Analysis (of Zillions and Zillions) of Images" (PAPARA(ZZ)I) (Marcon and Purser 2017). All Holothuroidea in non-overlapping pictures were first annotated by morphotype. Subsequently, morphotypes were identified to family, genus, or species level by an expert deep-sea Holothuroidea taxonomist (A. Gebruk). Reference was made to Bluhm and Gebruk (1999) and the "Atlas of Abyssal Megafauna Morphotypes of the Clipperton-Clarion Fracture Zone" (ccfzatlas.com). In PAPARA(ZZ)I body length and body width were measured for all Holothuroidea which lay straight using as reference for scaling a set of three laser points on the sea floor that formed an equilaterial triangle of 0.5 m.

Assessment of total sediment community oxygen consumption and holothuroidea community respiration

The sediment community oxygen consumption (SCOC) was measured in situ at the DISCOL reference site by deploying a benthic chamber lander (KUM GmbH, Germany) that was equipped with HydroFlash™ O_2 (Kongsberg Maritime Contros GmbH, Germany) optodes. After deployment of the lander, incubation chambers (20 × 20 × 20 cm) were slowly pushed into the sediment after which the oxygen concentration inside the chambers was continuously recorded over a period of 3 d (Boetius 2015). From the linear decrease in oxygen concentration, the oxygen consumption rate was estimated.

Holothuroidea community respiration was calculated based on abundance (see above) and in situ respiration rates of 13 individual Holothuroidea sampled during RV *Sonne* cruise 242-2 (A. Brown et al. unpubl.). Briefly, the "benthic incubation chamber system 3" (BICS3) (Hughes et al. 2011) was attached to the GEOMAR Ocean elevator (Linke 2010)

19395590, 2018, 5, Downloaded from https://aslopubs.onlinelibrary.wiley.com/doi/10.1002/lno.10929 by University Of Chemistry And, Wiley Online Library on [01/10/2026]. See the Terms and Conditions (https://onlinelibrary.wiley.com/terms-and-conditions) on Wiley Online Library for rules of use; OA articles are governed by the applicable Creative Commons License

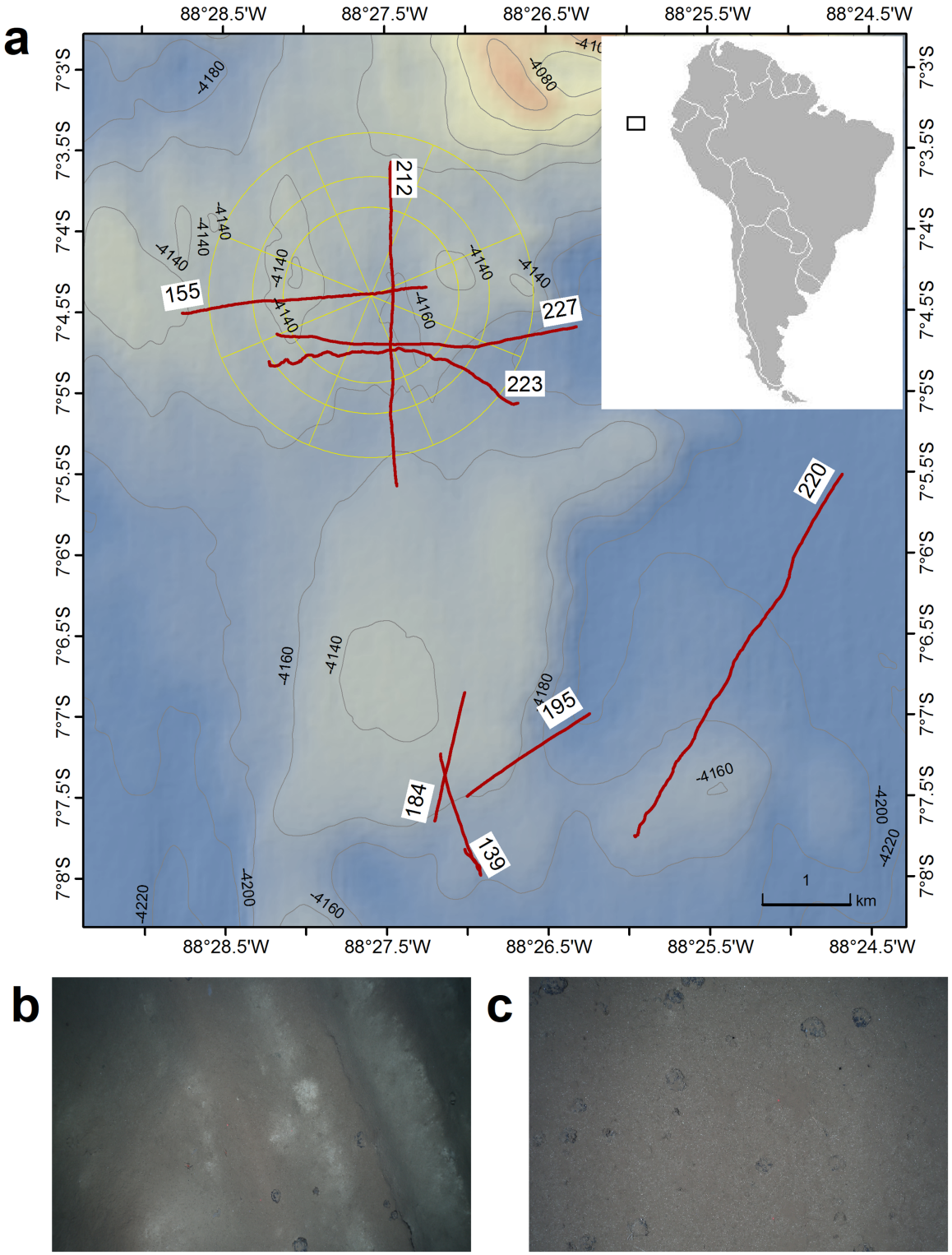

Fig. 1. (**a**) Map of the Peru Basin with bottom transects of all ocean floor observation system (OFOS) deployments inside the DISCOL experimental area (DEA, yellow circle) and at the southern and southeastern reference site. The number on white background correspond to the site numbers in Table 1. The black rectangle in the inserted map shows the exact location of DEA, but is unscaled. (**b**) Photograph of plough marks in the sediment at the DISCOL experimental area. (**c**) Photograph of seafloor at the reference site.

19395590, 2018, 5, Downloaded from https://aslopubs.onlinelibrary.wiley.com/doi/10.1002/lno.10929 by University Of Chemistry And, Wiley Online Library on [01/10/2026]. See the Terms and Conditions (https://onlinelibrary.wiley.com/terms-and-conditions) on Wiley Online Library for rules of use; OA articles are governed by the applicable Creative Commons License

Table 1. Ocean floor observation system (OFOS) transects. For each disturbance level (undisturbed, disturbed, and reference) photos of four OFOS transects were analyzed (Ref S = reference south; Ref SE = reference southeast; Dist. = disturbed within DEA; Undist. = undisturbed within DEA). As both disturbed and undisturbed within DEA photo sets originate from the same bottom tracks, the only difference between the photos was the presence of visible plough marks in the images.

OFOS transect	Start of bottom transect	End of bottom transect	Usable photos	Seafloor area imaged (m^2)	Disturbance level
139	7°07.71′S, 8°826.92′W	7°07.24′S, 8°827.16′W	87	418.0	Ref S
184	7°07.65′S, 8°827.20′W	7°06.86′S, 8°827.01′W	408	2069.0	Ref S
195	7°07.49′S, 8°827.00′W	7°06.98′S, 8°826.22′W	494	3015.7	Ref S
220	7°07.75′S, 8°825.96′W	7°05.76′S, 8°824.83′W	983	5434.7	Ref SE
155	7°04.50′S, 8°828.74′W	7°04.35′S, 8°827.36′W	498	2901.5	Dist.
212	7°05.57′S, 8°827.42′W	7°03.57′S, 8°827.46′W	792	390.4	Dist.
223	7°04.81′S, 8°828.21′W	7°05.06′S, 8°826.67′W	156	797.4	Dist.
227	7°04.65′S, 8°827.99′W	7°04.60′S, 8°826.36′W	392	1957.7	Dist.
155	7°04.50′S, 8°828.74′W	7°04.35′S, 8°827.25′W	338	2062.5	Undist.
212	7°05.57′S, 8°827.42′W	7°03.58′S, 8°827.45′W	473	2439.5	Undist.
223	7°04.80′S, 8°828.21′W	7°05.07′S, 8°826.71′W	676	3610.7	Undist.
227	7°04.63′S, 8°828.16′W	7°04.60′S, 8°826.33′W	435	2508.0	Undist.

and lowered to the seafloor. Holothuroidea were collected individually with the ROV Kiel 6000 and placed individually in three respiration chambers. The forth respiration chamber was kept empty as a control. After a Holothuroidea was placed in a chamber, the lid was closed immediately and oxygen consumption was measured over a period of at least 70 h (84.8 ± 14.3 h), with the empty chamber being used to assess the oxygen consumption rate of bottom seawater. Afterwards, the elevator platform with the BICS3 was brought to the surface, the Holothuroidea were collected and body length and width of each specimen were measured.

For the conversion of body length and width of individual Holothuroidea annotated on the OFOS photos into individual respiration rates, the body volume of the 13 Holothuroidea specimens (*Amperima* sp., *Benthodytes* sp., *Benthodytes typica*, *Mesothuria* sp., *Peniagone* sp. 2 (benthopelagic), *Synallactidae* gen. sp. 2) collected inside DEA was related to background-corrected respiration rates (measured originally in mmol O_2 ind^{-1} d^{-1}, A. Brown et al. unpubl.), but converted to mmol C ind^{-1} d^{-1} assuming a respiratory quotient of 1). The body volume of the 13 Holothuroidea specimens was calculated as the body length × body width^2. This formed the basis of the linear regression analysis of body volume vs. background-corrected respiration rates for all individual organisms (respiration rate = 9.00×10^{-5} × body length × body width^2; $n = 13$, $r^2 = 0.41$, $p \leq 0.001$). Subsequently, body length and width measurements of Holothuroidea from the OFOS pictures were converted into respiration rates following the equation given above whenever the organisms laid straight. When the length could not be measured, e.g., when the specimen was in a curved position, an average size for that specific morphotype was taken. The respiration per unit area was calculated as the sum of individual respiration rates divided by the area for which Holothuroidea abundance was determined.

Data analysis

For the Holothuroidea dataset after 26 yr, the univariate diversity indices Shannon index H' and Pielou index J' were calculated following Magurran (2004) using the "vegan" package in *R* (Oksanen et al. 2017). Analysis of similarities in assemblage composition of Holothuroidea was based on square-root transformed faunal density data using the ANOSIM

19395590, 2018, 5, Downloaded from https://aslopubs.onlinelibrary.wiley.com/doi/10.1002/lno.10929 by University Of Chemistry And, Wiley Online Library on [01/10/2026]. See the Terms and Conditions (https://onlinelibrary.wiley.com/terms-and-conditions) on Wiley Online Library for rules of use; OA articles are governed by the applicable Creative Commons License

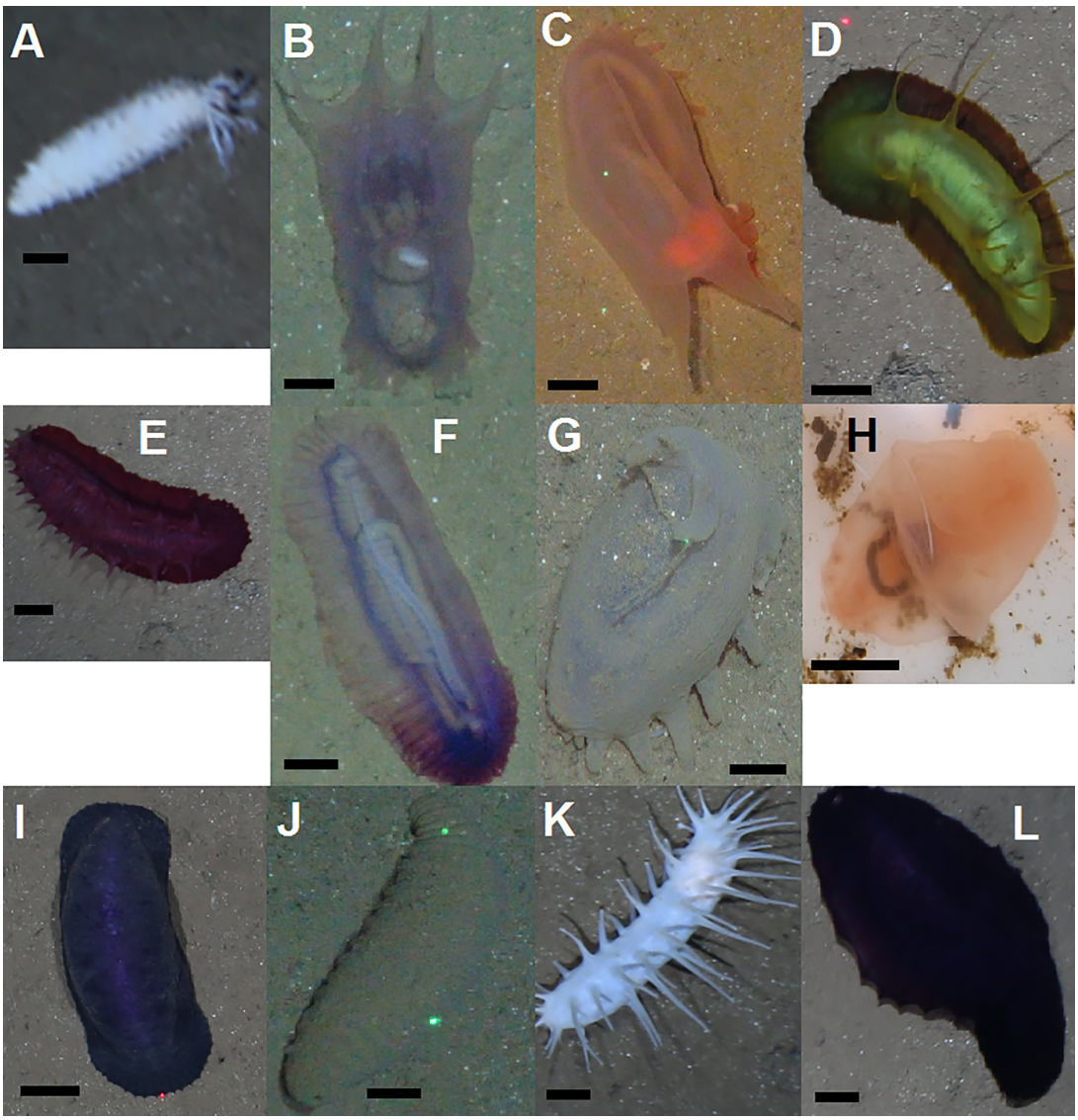

Fig. 2. Images of Holothuroidea morphotypes used in the present study: (**A**) *Abyssocucumis abyssorum*, (**B**) *Elpidiidae* gen. sp. 1 [= *Achlyoinice* sp. in Bluhm and Gebruk (1999)], (**C**) *Amperima* sp., (**D**) *Benthodytes gosarsi*, (**E**) *Benthodytes* sp., (**F**) *Benthodytes typica*, (**G**) *Elpidiidae* gen. sp. 2 ("double velum" morphotype in ccfzatlas.com), (**H**) *Elpidiidae* gen. sp. 3, (**I**) *Benthothuria* sp., (**J**) *Mesothuria* sp., (**K**) *Oneirophanta* sp., (**L**) *Galatheathuria* sp., (**M**) *Peniagone* sp. (= morphotype "palmata" in ccfzatlas.com), (**N**) *Peniagone* sp. 1, (**O**) *Peniagone* sp. 2 (benthopelagic), (**P**) *Psychronaetes hanseni*, (**Q**) *Psychropotes depressa*, (**R**) *Psychropotes longicauda*, (**S**) *Bathyplotes* sp., (**T**) *Synallactidae* gen. sp. 1, (**U**) *Synallactidae* gen. sp. 2, (**V**) *Synallactes profundi*, (**W**) *Synallactes* sp. (morphotype "pink" in ccfzatlas.com). The black bar represents 1 cm length. Photographs (**A**, **C**–**F**, **I**, **K**–**M**, **P**–**W**) from AWI; (**B**, **G**, **J**, **N**) from ROV Kiel 6000, Geomar; (**H**, **O**) from T. Stratmann. (Continued on next page).

routine in PRIMER6 (Clarke and Warwick 2008). The contribution of individual morphotypes to the similarity or dissimilarity between sites was calculated with the SIMPER routine in PRIMER6.

Differences in H' and J' indices, Holothuroidea densities, and respiration rates among disturbance levels (disturbed site, undisturbed site, reference site) were tested with One-Way ANOVA using the open-source software *R* (R Core Team 2016).

The Holothuroidea population densities were also analyzed over time (i.e., pre-disturbance −0.1, 0.1, 0.5, 3, 7 and 26 yr post-DISCOL disturbance) at disturbed, undisturbed and reference sites. The raw Holothuroidea density data from the earlier cruises were taken from Annex 2.08 in Bluhm (2001) and combined with the Holothuroidea density data of the present study. This resulted in an $n = 6$ for DISCOL1/1 (reference site), $n = 4$ and $n = 5$ for DISCOL 1/2 (disturbed and undisturbed site, respectively), $n = 3$, $n = 4$, and $n = 2$ for DISCOL 2 (disturbed, undisturbed, and reference site, respectively), $n = 4$, $n = 4$, and $n = 3$ for DISCOL 3, $n = 4$, $n = 4$, and $n = 5$ for ECOBENT and $n = 4$, $n = 4$, and $n = 4$ for DISCOL revisited. An unweighted One-Way ANOVA on the $\log_{10}$-transformed Holothuroidea density data was applied to

19395590, 2018, 5, Downloaded from https://aslopubs.onlinelibrary.wiley.com/doi/10.1002/lno.10929 by University Of Chemistry And, Wiley Online Library on [01/10/2026]. See the Terms and Conditions (https://onlinelibrary.wiley.com/terms-and-conditions) on Wiley Online Library for rules of use; OA articles are governed by the applicable Creative Commons License

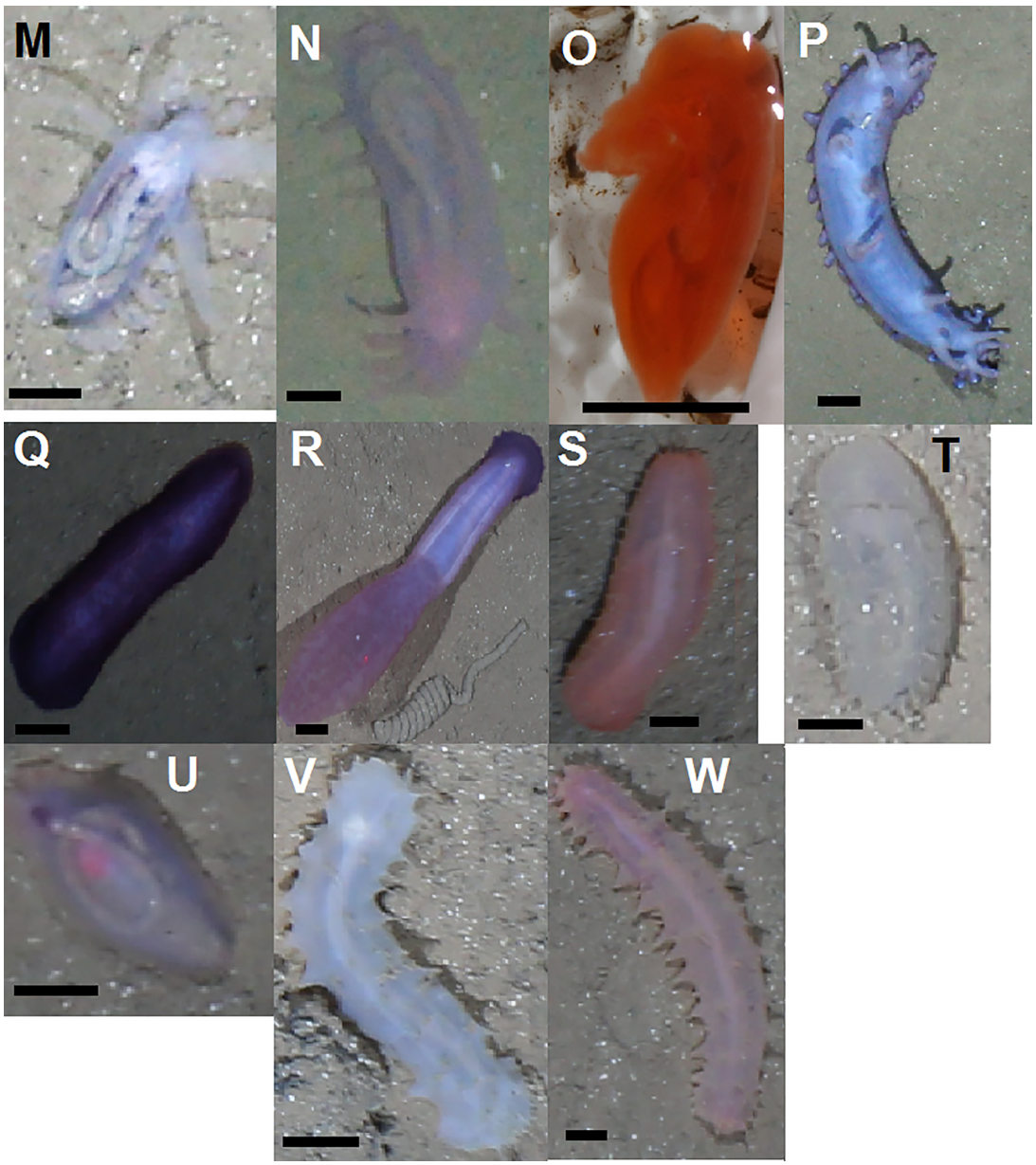

Fig. 2. Continued.

compare differences in Holothuroidea densities from disturbed, undisturbed, and reference sites of the same year.

Results are expressed as mean ± SD if not stated otherwise.

Results

Holothuroidea population density and community composition

A total of 23 different Holothuroidea morphotypes were identified from the full image set (Fig. 2). Where image quality was insufficient to identify morphotype, Holothuroidea were classified as "unknown Holothuroidea." A total of 22 morphotypes were found at the disturbed sites, including single records of *Abyssocucumis abyssorum* and *Galatheaturia* sp., 20 morphotypes at undisturbed sites, including a single record of *Benthodytes gosarsi*, and 17 morphotypes at the reference sites (Fig. 3). The most abundant species were *Amperima* sp., *Benthodytes typica*, and *Mesothuria* sp. (Fig. 3; Table 2), which together contributed 46% ± 6% to the total density. However, their ranking in species abundance varied among sites (Fig. 3).

The density of Holothuroidea did not differ among sites (ANOVA: $F_{2,9} = 0.042$, $p = 0.96$) with mean densities (ind. ha^{-1}) of 241 ± 51 at the disturbed site, 240 ± 40 at the

19395590, 2018, 5, Downloaded from https://aslopubs.onlinelibrary.wiley.com/doi/10.1002/lno.10929 by University Of Chemistry And, Wiley Online Library on [01/10/2026]. See the Terms and Conditions (https://onlinelibrary.wiley.com/terms-and-conditions) on Wiley Online Library for rules of use; OA articles are governed by the applicable Creative Commons License

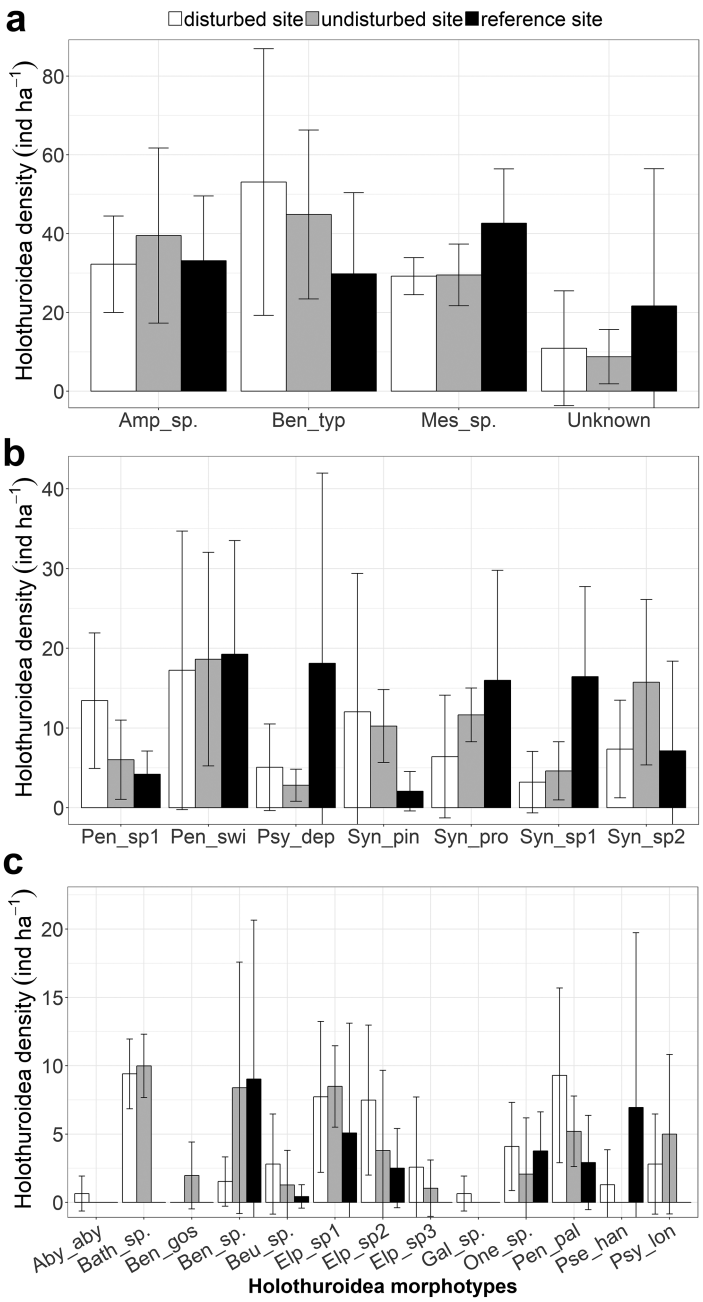

Fig. 3. Holothuroidea morphotype densities > 60 ind. ha^{-1} (**a**), > 40 ind. ha^{-1} (**b**), and > 10 ind. ha^{-1} (**c**) in the three areas disturbed within DEA, undisturbed within DEA, and reference, shown as mean values with standard deviations. Abbreviations: Aby_aby = *Abyssocucumis abyssorum*, Amp_sp. = *Amperima* sp., Bath_sp. = *Bathyplotes* sp., Ben_gos = *Benthodytes gosarsi*, Ben_sp. = *Benthodytes* sp., Ben_typ = *Benthodytes typica*, Beu_sp. = *Benthothuria* sp., Elp_sp1 = Elpidiidae gen. sp. 1 [= *Achlyoinice* sp. in Bluhm and Gebruk (1999)], Elp_sp2 = *Elpidiidae* gen. sp. 2 ("double velum" morphotype in ccfzatlas.com), Elp_sp3 = *Elpidiidae* gen. sp. 3, Gal_sp. = *Galatheathuria* sp., Mes_sp. = *Mesothuria* sp., One_sp. = *Oneirophanta* sp., Pen_pal = *Peniagone* sp. (= morphotype "palmate" in ccfzatlas.com), Pen_sp1 = *Peniagone* sp. 1, Pen_swi = *Peniagone* sp. 2 (benthopelagic), Pse_han = *Psychronaetes hanseni*, Psy_dep = *Psychropotes depressa*, Psy_lon = *Psychropotes longicauda*, Syn_pin = *Synallactes* sp. (morphotype "pink" in ccfzatlas.com), Syn_pro = *Synallactes profundi*, Syn_sp1 = *Synallactidae* gen. sp. 1, Syn_sp2 = *Synallactidae* gen. sp. 2, Unknown = Unknown Holothurian.

undisturbed site, and 241 ± 33 at the reference site. There were no differences in mean density of each morphotype among sites (ANOSIM: $R = 0.019$, $p = 0.39$), either. Similarity in species composition among sites was driven by *Benthodytes typica* (contribution to similarity between disturbed and undisturbed sites: 10.46–16.28%), *Amperima* sp. (10.49%), and the group of unknown Holothuroidea (10.28% and 10.54%). The Shannon diversity index H' and Pielou evenness index J' did

19395590, 2018, 5, Downloaded from https://aslopubs.onlinelibrary.wiley.com/doi/10.1002/lno.10929 by University Of Chemistry And, Wiley Online Library on [01/10/2026]. See the Terms and Conditions (https://onlinelibrary.wiley.com/terms-and-conditions) on Wiley Online Library for rules of use; OA articles are governed by the applicable Creative Commons License

Table 2. Density (ind. ha^{-1}) and respiration ($\times 10^{-3}$ mmol C m^{-2} d^{-1}) of the three most abundant Holothuroidea taxa for each location (Ref S = reference south; Ref SE = reference southeast; Dist. = disturbed within DEA; Undist. = undisturbed within DEA).

OFOS transect	Disturbance level	*Benthodytes typica*		*Amperima* sp.		*Mesothuria* sp.	
		Density	Respiration	Density	Respiration	Density	Respiration
139	Ref S	Not seen		52	0.22	52	0.06
184	Ref S	34	0.14	25	0.07	49	0.05
195	Ref S	47	0.27	41	0.12	41	0.05
220	Ref SE	38	0.29	15	0.06	22	0.04
155	Dist.	28	0.20	25	0.08	35	0.02
212	Dist.	62	0.43	28	0.11	26	0.03
223	Dist.	25	0.16	50	0.22	25	0.46
227	Dist.	97	0.63	26	0.11	31	0.06
155	Undist.	20	0.09	66	0.32	25	0.05
212	Undist.	70	0.33	50	0.29	41	0.07
223	Undist.	36	0.26	25	0.13	25	0.07
227	Undist.	53	0.43	18	0.10	26	0.06

Table 3. Holothuroidea density (ind. ha^{-1}), respiration ($\times 10^{-3}$ mmol C m^{-2} d^{-1}) and density based diversity metrics (H': Shannon Index; J': Pielou's evenness) for each location (Ref S = reference south; Ref SE = reference southeast; Dist. = disturbed within DEA; Undist. = undisturbed within DEA).

OFOS transect	Disturbance level	Density	Respiration	H'	J'
139	Ref S	261	0.60	1.89	0.59
184	Ref S	230	0.46	2.30	0.72
195	Ref S	274	0.66	2.33	0.73
220	Ref SE	200	0.62	2.00	0.63
Mean ± SD	Ref	241 ± 33	0.58 ± 0.09	2.13 ± 0.22	0.67 ± 0.07
155	Dist.	183	0.45	2.38	0.75
212	Dist.	293	1.04	2.69	0.85
223	Dist.	214	0.66	2.07	0.65
227	Dist.	272	1.06	2.19	0.69
Mean ± SD	Dist.	241 ± 51	0.80 ± 0.30	2.33 ± 0.27	0.74 ± 0.09
155	Undist.	233	0.71	2.30	0.72
212	Undist.	297	0.92	2.44	0.77
223	Undist.	226	0.74	2.60	0.82
227	Undist.	203	0.73	2.34	0.74
Mean ± SD	Undist.	240 ± 40	0.77 ± 0.10	2.42 ± 0.13	0.76 ± 0.04

not differ significantly among sites, either (ANOVA for H': $F_{2,9} = 1.914$, $p = 0.20$; ANOVA for J': $F_{2,9} = 2.027$, $p = 0.19$; Table 3).

Holothuroidea density changes over time

The holothurian mean density of 142 ± 37 ind. ha^{-1} of the pre-disturbance study in February 1989 dropped by 87% (18 ± 10 ind. ha^{-1}) at the disturbed site and by 39% (86 ± 31 ind. ha^{-1}) at the undisturbed site immediately after the disturbance (Fig. 4; Bluhm 2001). This difference in mean Holothuroidea densities between disturbed and undisturbed site 0.1 yr post DISCOL disturbance was statistical significant (ANOVA: $F_{1,7} = 26.23$, $p = 0.001$) and persisted until half a year after the DISCOL disturbance (ANOVA: $F_{2,6} = 16.46$, $p = 0.004$) (Bluhm 2001). Three years after the DISCOL disturbance, Holothuroidea mean densities at the disturbed site (99 ± 54 ind. ha^{-1}) were 37% of the mean densities at the undisturbed site (266 ± 200 ind. ha^{-1}; Bluhm 2001), but the difference between disturbance levels was not significant anymore due to a large variability among the OFOS tracks (ANOVA: $F_{2,8} = 4.18$, $p = 0.06$).

19395590, 2018, 5, Downloaded from https://aslopubs.onlinelibrary.wiley.com/doi/10.1002/lno.10929 by University Of Chemistry And, Wiley Online Library on [01/10/2026]. See the Terms and Conditions (https://onlinelibrary.wiley.com/terms-and-conditions) on Wiley Online Library for rules of use; OA articles are governed by the applicable Creative Commons License

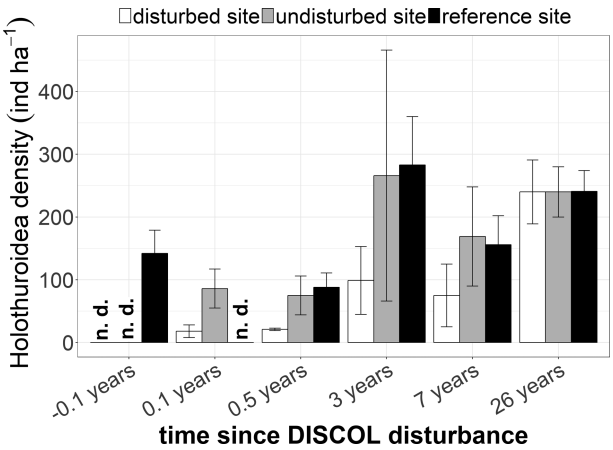

Fig. 4. Holothuroidea densities measured during all previous post-disturbance DISCOL cruises at the disturbed as well as undisturbed sites, and, pre- and post-impact in the reference areas (no data were available for the cruise 0.1 yr after ploughing). Data from pre-disturbance (–0.1 yr), 0.1 yr, 0.5 yr, 3 yr, and 7 yr after the DISCOL experiment were taken from Bluhm (2001) annex 2.08. n. d. means that no data were available for this specific disturbance and year (disturbed and undisturbed site at −0.1 yr; reference at 0.1 yr).

Holothuroidea community respiration

Holothuroidea community respiration ($\times 10^{-3}$ mmol C m^{-2} d^{-1}) was not significantly different among the reference sites (0.58 ± 0.09), undisturbed (0.77 ± 0.10), and disturbed sites (0.80 ± 0.30) (ANOVA: $F_{2,9} = 1.591$, $p = 0.256$).

Discussion

Deep-sea mining for polymetallic nodules will impact the benthic ecosystem in various ways (Jones et al. 2017) and it is therefore vital to estimate how long it may take for ecosystems to recover from the resultant seafloor disturbances (Gollner et al. 2017). Data presented here demonstrate that Holothuroidea population density, community composition, and respiration have recovered 26 yr after a sediment disturbance event in the Peru Basin. We here discuss the mechanisms involved in the recovery of Holothuroidea composition and functioning following the experimental disturbance and consider these in the context of future deep-sea mining activities.

Holothuroidea assemblage and densities

Holothuroidea assemblages in abyssal plains are often dominated by a few species, such as *Amperima rosea*, *Oneirophanta mutabilis*, *Psychropotes longicauda*, and *Pseudostichopus villosus* at the Porcupine Abyssal Plain (PAP, north-east Atlantic; Billett et al. 2001, 2010) or *Abyssocucumis abyssorum*, *Peniagone vitrea*, and *Elpidia minutissima* at Station M in the north-east Pacific (Smith et al. 1993). The Holothuroidea assemblage in the Peru Basin therefore resembles a typical deep-sea community, where *Amperima* sp., *Benthodytes typica*, and *Mesothuria* sp. comprise almost 50% of the total Holothuroidea.

A key finding of this study is that Holothuroidea density and community composition recovered from a disturbance after 26 yr. These results are in contrast with a study on megafaunal recovery from the CCZ, where isolated individual disturbance tracks still showed reduced Holothuroidea densities up to 37 yr after the disturbance (Vanreusel et al. 2016). This discrepancy may be a result of various factors, including temporal variability in Holothuroidea abundance, different disturbance methods and scales, and/or differences in the food supply to the CCZ compared to the DISCOL area.

The abundance of particular mobile abyssal megafauna taxa can fluctuate inter-annually by one to three orders of magnitude (Ruhl 2007). For example, the density of the Holothuroidea *Amperima rosea* increased by more than two orders of magnitude at the Porcupine Abyssal Plain (PAP, NE Atlantic) during the famous "Amperima event" (Billett et al. 2001, 2010), likely in response to increased food supply to the seafloor. Hence, photo transects performed at a particular time only represent a snapshot of the megafaunal assemblage and do not show potential temporal variability. Holothuroidea abundance in a comparatively narrow and short mining track (Vanreusel et al. 2016) where the number of individual specimen observed is likely very low is especially prone to such spatial and temporal sampling bias.

Another key difference between the CCZ and DISCOL studies is the imposed disturbance method. During the DISCOL experiment the upper sediment layer was mixed in a ~ 2.4 km^2 area (22% of 10.8 km^2 DEA; Thiel and Schriever 1989) leaving a mosaic of dark-brown sediment and greyish clay (Fig. 1b). In contrast, the disturbance at the CCZ involved complete removal of the upper 5 cm of sediment in individual 2.5 m wide tracks (Khripounoff et al. 2006). Surface sediments in the CCZ contain about 0.48% organic carbon (per dry sediment), whereas the carbon content in sediments below 5 cm in the CCZ is only 0.35% (Khripounoff et al. 2006). Hence, food availability in the CCZ tracks were reduced which may have contributed to the lower abundances. Other potential causes could be changes in water content with sediment depth (Grupe et al. 2001), differences in sediment compactness, sediment grain size, terrain, or texture of the surface sediment in the tracks. Finally, the investigated site at the north-western CCZ is more oligotrophic as compared to the DISCOL site, with a particulate organic carbon (POC) flux estimated to be 1.5 mg C_{org} m^{-2} d^{-1} (Vanreusel et al. 2016). The flux of particulate organic carbon in the Peru Basin is higher, with model estimates of 3.86 mg C_{org} m^{-2} d^{-1} (Haeckel et al. 2001). Consequently, re-establishing food availability in tracks following disturbance will likely differ between the CCZ and the Peru Basin, because of differences in disturbance method and trophic status.

Holothuroidea respiration

The total Holothuroidea respiration at the DISCOL site (0.01 mg O_2 m^{-2} d^{-1}) was comparable to, but at the lower

19395590, 2018, 5, Downloaded from https://aslopubs.onlinelibrary.wiley.com/doi/10.1002/lno.10929 by University Of Chemistry And, Wiley Online Library on [01/10/2026]. See the Terms and Conditions (https://onlinelibrary.wiley.com/terms-and-conditions) on Wiley Online Library for rules of use; OA articles are governed by the applicable Creative Commons License

end of the echinoderm respiration calculated for PAP (respiration range: 0.01–0.04 mg O_2 m^{-2} d^{-1}; Ruhl et al. 2014) and one order of magnitude lower than the absolute echinoderm respiration calculated for Station M (respiration range: 0.15–0.65 mg O_2 m^{-2} d^{-1}; Ruhl et al. 2014). The latter difference can be attributed to the dominance of non-Holothuroidea echinoderms to the total echinoderm respiration at Station M. When only the total respiration rate of the dominant species *Ophiuroidea*, *Elpidia* spp., and *Echinocrepis rostrata* (Ruhl et al. 2014) was considered, the Holothuroidea respiration at Station M was in the same order of magnitude as the Peru Basin taking into account the overall higher Holothuroidea densities in the northeast Pacific than in the southeast Pacific (Ruhl 2007; Ruhl et al. 2014).

The relative contribution of Holothuroidea to the total benthic respiration depends on the supply of POC to the system (Ruhl et al. 2014). In food-limited abyssal plains such as at Station M, model estimates indicated that Holothuroidea contribute between 1.44% and 2.42% to the total community respiration (Dunlop et al. 2016). In the present study, the Holothuroidea contributed even less to the total benthic respiration with an estimated 0.18% of the community respiration of 114.98 ± 12.90 mmol O_2 m^{-2} yr^{-1}.

Holothuroidea recovery over time

Most Holothuroidea are mobile and move over the sediment or engage in swimming behavior (Miller and Pawson 1990; Kaufmann and Smith 1997; Jamieson et al. 2011; Rogacheva et al. 2012). Assuming a unidirectional movement of 10 cm h^{-1} and 65 cm h^{-1} (Kaufmann and Smith 1997), Holothuroidea would need approximately 0.66 yr to cross the entire DEA, of which only 22% was directly denuded of Holothuroidea (Thiel and Schriever 1989). Even though Holothuroidea species alternate between unidirectional movement, a run-and-mill strategy and loops (Kaufmann and Smith 1997), recolonization based on movement alone can be expected within a year. Hence, the recovery period reported in this study (3 yr for a partial recovery and $>$20 yr for full recovery) are comparatively long, which warrants further consideration.

Deposit-feeding Holothuroidea depend on organic compounds from the sediment (Amaro et al. 2010) and some species feed selectively on fresh organic detritus (FitzGeorge-Balfour et al. 2010) and pigment-rich organic matter (Hudson et al. 2005). Additionally, movement activity of Holothuroidea has been linked to their search for patchily-distributed high-quality organic resources, including fresh phytodetritus (Smith et al. 1997). Food conditions in the disturbance tracks are thought to be unfavorable due to a dilution of high-quality organic matter by the ploughing disturbance (e.g., protein concentrations half a year post-disturbance at undisturbed sites: 6.86 ± 3.59 g protein m^{-2} and at disturbed sites: 3.59 ± 1.53 g protein m^{-2}; Forschungsverbund Tiefsee-Umweltschutz, unpubl.). Hence, one would expect that Holothuroidea will respond to these poorer food conditions by active emigration out of the disturbance tracks, leaving their densities in the disturbance tracks reduced compared to the surrounding sediments (i.e., undisturbed and reference sites). So, even though Holothuroidea have the capacity to recolonize the disturbed area in due time, recolonization may lag behind due to unfavorable food conditions. We speculate that this may explain the relatively long recovery periods found in our study. However, holothurians also select for the finer sediment particle fraction (Khripounoff and Sibuet 1980) and therefore a change in the sediment particle size and composition in disturbance tracks could reduce the recolonization speed as well.

Outlook to deep-sea mining impacts

We found that Holothuroidea abundance, community composition, and respiration activity recovered from a small-scale disturbance event in the Peru Basin on an annual to decadal scale. However, the results of this study cannot be directly extrapolated to mining scenarios, because they describe the recovery of one mobile conspicuous taxon and other taxonomic groups, especially those of sessile organisms, will have very different recovery rates. The recovery also occurred in a relatively lightly disturbed area of only 10.8 km^2, whereas a single mining operation will likely remove polymetallic nodules over an area between 300 km^2 and $>$1000 km^2 (Smith et al. 2008; Levin et al. 2016). The type of disturbance examined here (sediment and nodules ploughing with little removal of the upper sediment) is also not representative of the actual disturbances, which will be associated with nodule and surface sediment removal (Thiel und Tiefsee-Umweltschutz 2001). Furthermore, the CCZ is a key target area for deep-sea mining and spans across a range of trophic settings, which may delay recovery, and potentially cumulative effects, such as overlapping mining plumes from nearby mining operations or climate change-related shifts in POC export fluxes (Levin et al. 2016; Sweetman et al. 2017; Yool et al. 2017) were not considered in this current study. Ultimately, to gain more knowledge about potential recovery rates of fauna after industrial-scale mining, a scientifically supported industrial test-mining operation in the CCZ is required, and all species of megafauna as well as all size classes of fauna should be monitored for several decades after resource extraction.

References

Ahnert, A., and G. Schriever. 2001. Response of abyssal Copepoda Harpacticoida (Crustacea) and other meiobenthos to an artificial disturbance and its bearing on future mining for polymetallic nodules. Deep-Sea Res. Part II **48**: 3779–3794. doi:10.1016/S0967-0645(01)00067-4

Amaro, T., S. Bianchelli, D. S. Billett, M. Cunha, A. Pusceddu, and R. Danovaro. 2010. The trophic biology of the holothurian *Molpadia musculus*: Implications for

19395590, 2018, 5, Downloaded from https://aslopubs.onlinelibrary.wiley.com/doi/10.1002/lno.10929 by University Of Chemistry And, Wiley Online Library on [01/10/2026]. See the Terms and Conditions (https://onlinelibrary.wiley.com/terms-and-conditions) on Wiley Online Library for rules of use; OA articles are governed by the applicable Creative Commons License

organic matter cycling and ecosystem functioning in a deep submarine canyon. Biogeosciences **7**: 2419–2432. doi:10.5194/bg-7-2419-2010

Amon, D. J., A. F. Ziegler, T. G. Dahlgren, A. G. Glover, A. Goineau, A. J. Gooday, H. Wiklund, and C. R. Smith. 2016. Insights into the abundance and diversity of abyssal megafauna in a polymetallic-nodule region in the eastern Clarion-Clipperton Zone. Sci. Rep. **6**: 30492. doi:10.1038/srep30492

Bett, B. J., M. G. Malzone, B. E. Narayanaswamy, and B. D. Wigham. 2001. Temporal variability in phytodetritus and megabenthic activity at the seabed in the deep Northeast Atlantic. Limnol. Oceanogr. **50**: 349–368. doi:10.1016/S0079-6611(01)00066-0

Billett, D. S., B. Bett, A. Rice, M. Thurston, J. Galéron, M. Sibuet, and G. Wolff. 2001. Long-term change in the megabenthos of the Porcupine Abyssal Plain (NE Atlantic). Prog. Oceanogr. **50**: 325–348. doi:10.1016/S0079-6611(01)00060-X

Billett, D. S., B. Bett, W. Reid, B. Boorman, and I. Priede. 2010. Long-term change in the abyssal NE Atlantic: The 'Amperima Event' revisited. Deep-Sea Res. Part II **57**: 1406–1417. doi:10.1016/j.dsr2.2009.02.001

Bluhm, H. 2001. Re-establishment of an abyssal megabenthic community after experimental physical disturbance of the seafloor. Deep-Sea Res. Part II **48**: 3841–3868. doi:10.1016/S0967-0645(01)00070-4

Bluhm, H., G. Schriever, and H. Thiel. 1995. Megabenthic recolonization in an experimentally disturbed abyssal manganese nodule area. Mar. Georesour. Geotechnol. **13**: 393–416. doi:10.1080/10641199509388295

Bluhm, H., and H. Thiel. 1996. Photographic and video surveys for large scale animal and seafloor surface charting aiming at ecological characterization of habitats and communities. Proceedings of the International Seminar on Deep Seabed Mining Technology, 18–20 October 1996. Peking, PR China: C15-C23.

Bluhm, H., and A. Gebruk. 1999. Holothuroidea (Echinodermata) of the Peru Basin-ecological and taxonomic remarks based on underwater images. Mar. Ecol. **20**: 167–195. doi:10.1046/j.1439-0485.1999.00072.x

Boetius, A. 2015. Cruise Report SO242/2: DISCOL revisited. JPI OCEANS Ecological Aspects of Deep-Sea Mining. Guayaquil: 28.08.2015–Guayaquil: 01.10.2015.

Borowski, C. 2001. Physically disturbed deep-sea macrofauna in the Peru Basin, southeast Pacific, revisited 7 years after the experimental impact. Deep-Sea Res. Part II **48**: 3809–3839. doi:10.1016/S0967-0645(01)00069-8

Borowski, C., and H. Thiel. 1998. Deep-sea macrofaunal impacts of a large-scale physical disturbance experiment in the Southeast Pacific. Deep-Sea Res. Part II **45**: 55–81. doi:10.1016/S0967-0645(97)00073-8

Brooke, S., M. Holmes, and C. Young. 2009. Sediment tolerance of two different morphotypes of the deep-sea coral *Lophelia pertusa* from the Gulf of Mexico. Mar. Ecol. Prog. Ser. **390**: 137–144. doi:10.3354/meps08191

Danovaro, R., M. Fabiano, and N. Della Croce. 1993. Labile organic matter and microbial biomasses in deep-sea sediments (Eastern Mediterranean Sea). Deep-Sea Res. Part I **40**: 953–965. doi:10.1016/0967-0637(93)90083-F

Danovaro, R., M. Fabiano, G. Albertelli, and N. D. Croce. 1995. Vertical distribution of meiobenthos in bathyal sediments of the eastern Mediterranean Sea: Relationship with labile organic matter and bacterial biomasses. Mar. Ecol. **16**: 103–116. doi:10.1111/j.1439-0485.1995.tb00398.x

De Leo, F. C., C. R. Smith, A. A. Rowden, D. A. Bowden, and M. R. Clark. 2010. Submarine canyons: Hotspots of benthic biomass and productivity in the deep sea. Proc. R. Soc. B **277**: 2783–2792. doi:10.1098/rspb.2010.0462

Dunlop, K. M., D. van Oevelen, H. A. Ruhl, C. L. Huffard, L. A. Kuhnz, and K. L. Smith. 2016. Carbon cycling in the deep eastern North Pacific benthic food web: Investigating the effect of organic carbon input. Limnol. Oceanogr. **61**: 1956–1968. doi:10.1002/lno.10345

Durden, J. M., and others. 2016. Perspectives in visual imaging for marine biology and ecology: From acquisition to understanding. Oceanogr. Mar. Biol. **54**: 1–72.

Fitzgeorge-Balfour, T., D. S. Billett, G. A. Wolff, A. Thompson, and P. A. Tyler. 2010. Phytopigments as biomarkers of selectivity in abyssal holothurians; interspecific differences in response to a changing food supply. Deep-Sea Res. Part II **57**: 1418–1428. doi:10.1016/j.dsr2.2010.01.013

Foell, E., H. Thiel, and G. Schriever. 1990. DISCOL: A long-term, large-scale, disturbance-recolonization experiment in the abyssal eastern tropical South Pacific Ocean. Offshore Technology Conference, 1990.

Foell, E., H. Thiel, and G. Schriever. 1992. DISCOL: A long-term, large-scale, disturbance-recolonization experiment in the abyssal eastern tropical South Pacific Ocean. Miner. Eng. **44**: 90–94.

Glasby, G. 2000. Lessons learned from deep-sea mining. Science **289**: 551–553. doi:10.1126/science.289.5479.551

Gollner, S., and others. 2017. Resilience of benthic deep-sea fauna to mining activities. Mar. Environ. Res. **129**: 76–101. doi:10.1016/j.marenvres.2017.04.010

Grupe, B., H. J. Becker, and H. U. Oebius. 2001. Geotechnical and sedimentological investigations of deep-sea sediments from a manganese nodule field of the Peru Basin. Deep-Sea Res. Part II **48**: 3593–3608. doi:10.1016/S0967-0645(01)00058-3

Haeckel, M., I. König, V. Riech, M. E. Weber, and E. Suess. 2001. Pore water profiles and numerical modelling of biogeochemical processes in Peru Basin deep-sea sediments. Deep-Sea Res. Part II **48**: 3713–3736. doi:10.1016/S0967-0645(01)00064-9

Hughes, S. J. M., H. A. Ruhl, L. E. Hawkins, C. Hauton, B. Boorman, and D. S. Billett. 2011. Deep-sea echinoderm oxygen consumption rates and an interclass comparison of metabolic rates in Asteroidea, Crinoidea, Echinoidea,

19395590, 2018, 5, Downloaded from https://aslopubs.onlinelibrary.wiley.com/doi/10.1002/lno.10929 by University Of Chemistry And, Wiley Online Library on [01/10/2026]. See the Terms and Conditions (https://onlinelibrary.wiley.com/terms-and-conditions) on Wiley Online Library for rules of use; OA articles are governed by the applicable Creative Commons License

Holothuroidea and Ophiuroidea. J. Exp. Biol. **214**: 2512–2521. doi:10.1242/jeb.055954

Jamieson, A. J., A. Gebruk, T. Fujii, and M. Solan. 2011. Functional effects of the hadal sea cucumber Elpidia atakama (Echinodermata: Holothuroidea, Elasipodida) reflect small-scale patterns of resource availability. Mar. Biol. **158**: 2695–2703. doi:10.1007/s00227-011-1767-7

Jankowski, J. A., and W. Zielke. 2001. The mesoscale sediment transport due to technical activities in the deep sea. Deep-Sea Res. Part II **48**: 3487–3521. doi:10.1016/S0967-0645(01)00054-6

Jones, D. O. B., and others. 2017. Biological responses to disturbance from simulated deep-sea polymetallic nodule mining. PLoS One **12**: e0171750. doi:10.1371/journal.pone.0171750

Kaufmann, R., and K. Smith. 1997. Activity patterns of mobile epibenthic megafauna at an abyssal site in the eastern North Pacific: Results from a 17-month time-lapse photographic study. Deep-Sea Res. Part I **44**: 559–579. doi:10.1016/S0967-0637(97)00005-8

Khripounoff, A., and M. Sibuet. 1980. La nutrition d'echinodermes abyssaux. I. Alimentation des holothuries. Mar. Biol. **60**: 17–26. doi:10.1007/BF00395602

Khripounoff, A., J.-C. Caprais, P. Crassous, and J. Etoubleau. 2006. Geochemical and biological recovery of the disturbed seafloor in polymetallic nodule fields of the Clipperton-Clarion Fracture Zone (CCFZ) at 5,000-m depth. Limnol. Oceanogr. **51**: 2033–2041. doi:10.4319/lo.2006.51.5.2033

Klein, G., E. Rachor, and S. A. Gerlach. 1975. Dynamics and productivity of two populations of the benthic tube-dwelling amphipod *Ampelisca brevicornis* (Costa) in Helgoland Bight. Ophelia **14**: 139–159. doi:10.1080/00785236.1975.10421973

Leitner, A. B., A. Neuheimer, E. Donlon, C. R. Smith, and J. C. Drazen. 2017. Environmental and bathymetric influences on abyssal bait-attending communities of the Clarion Clipperton Zone. Deep-Sea Res. Part I **125**: 65–80. doi:10.1016/j.dsr.2017.04.017

Levin, L. A., and others. 2016. Defining "serious harm" to the marine environment in the context of deep-seabed mining. Mar. Policy **74**: 245–259. doi:10.1016/j.marpol.2016.09.032

Linke, P. 2010. Cruise Report SO-210: ChiFlux. Identification and investigation of fluid flux, mass wasting and sediments in the forearc of the central Chilean subduction zone. Valparaiso: 23.09.2010–Valparaiso: 01.11.2010. GEOMAR Helmholtz-Zentrum für Ozeanforschung Kiel.

Magurran, A. E. 2004. Measuring biological diversity. Blackwell Science Ltd.

Marchig, V., U. von Stackelberg, H. Hufnagel, and G. Durn. 2001. Compositional changes of surface sediments and variability of manganese nodules in the Peru Basin. Deep-Sea Res. Part II **48**: 3523–3547. doi:10.1016/S0967-0645(01)00055-8

Marcon, Y., and A. Purser. 2017. PAPARA (ZZ) I: An open-source software interface for annotating photographs of the deep-sea. SoftwareX **6**: 69–80. doi:10.1016/j.softx.2017.02.002

Miller, J. E., and D. L. Pawson. 1990. Swimming sea cucumbers (Echinodermata: Holothuroidea): A survey, with analysis of swimming behavior in four bathyal species. Smithson. Contrib. Mar. Sci. 35: 1–18. doi:10.5479/si.01960768.35.1

Oebius, H. U., H. J. Becker, S. Rolinski, and J. A. Jankowski. 2001. Parameterization and evaluation of marine environmental impacts produced by deep-sea manganese nodule mining. Deep-Sea Res. Part II **48**: 3453–3467. doi:10.1016/S0967-0645(01)00052-2

Oksanen, J., and others. 2017. vegan: Community Ecology Package. R package version 2.4-3. Available from https://CRAN.R-project.org/package=vegan

Purser, A., Y. Marcon, H.-J. T. Hoving, M. Vecchione, U. Piatkowski, D. Eason, H. Bluhm, and A. Boetius. 2016. Association of deep-sea incirrate octopods with manganese crusts and nodule fields in the Pacific Ocean. Curr. Biol. **26**: R1247–R1271. doi:10.1016/j.cub.2016.10.052

R Core Team. 2016. R: A language and environment for statistical computing. R Foundation for Statistical Computing, Vienna, Austria. Available from https://www.R-project.org/

Rogacheva, A., A. Gebruk, and C. H. Alt. 2012. Swimming deep-sea holothurians (Echinodermata: Holothuroidea) on the northern Mid-Atlantic Ridge. Zoosymposia **7**: 213–224. doi:10.11646/zoosymposia.7.1.19

Ruhl, H. A. 2007. Abundance and size distribution dynamics of abyssal epibenthic megafauna in the northeast Pacific. Ecology **88**: 1250–1262. doi:10.1890/06-0890

Ruhl, H. A., and others. 2014. Links between deep-sea respiration and community dynamics. Ecology **95**: 1651–1662. doi:10.1890/13-0675.1

Schriever, G., A. Koschinsky, and H. Bluhm. 1996. Cruise Report ATESEPP. Auswirkungen technischer Eingriffe in das Ökosystem der Tiefsee im Süd-Ost-Pazifik vor Peru. (Impacts of potential technical interventions on the deep-sea ecosystem of the southeast Pacific off Peru). Sonne Cruise 106. January 1–March 9, 1996 Balboa/Panama – Balboa/Panama. Berichte aus dem Zentrum für Meeres- und Klimaforschung. Reihe E: Hydrobiologie und Fischereiwissenschaft Nr. 11. Institut für Hydrobiologie und Fischereiwissenschaft Hamburg.

Smallwood, B. J., G. A. Wolff, B. J. Bett, C. R. Smith, D. Hoover, J. D. Gage, and A. Patience. 1999. Megafauna can control the quality of organic matter in marine sediments. Naturwissenschaften **86**: 320–324. doi:10.1007/s001140050624

Smith, A., J. Matthiopoulos, and I. G. Priede. 1997. Areal coverage of the ocean floor by the deep-sea elasipodid holothurian *Oneirophanta mutabilis*: Estimates using systematic, random and directional search strategy

19395590, 2018, 5, Downloaded from https://aslopubs.onlinelibrary.wiley.com/doi/10.1002/lno.10929 by University Of Chemistry And, Wiley Online Library on [01/10/2026]. See the Terms and Conditions (https://onlinelibrary.wiley.com/terms-and-conditions) on Wiley Online Library for rules of use; OA articles are governed by the applicable Creative Commons License

simulations. Deep-Sea Res. Part I **44**: 477–486. doi: 10.1016/S0967-0637(96)00112-4

Smith, C. R., L. A. Levin, A. Koslow, P. A. Tyler, and A. G. Glover. 2008. The near future of the deep seafloor ecosystem, p. 334–352. *In* N. Polunin [ed.], Aquatic ecosystems: Trends and global prospects. Cambridge Univ. Press.

Smith, K. L., R. Kaufmann, and W. Wakefield. 1993. Mobile megafaunal activity monitored with a time-lapse camera in the abyssal North Pacific. Deep-Sea Res. Part I **40**: 2307–2324. doi:10.1016/0967-0637(93)90106-D

Sweetman, A. K., and others. 2017. Major impacts of climate change on deep-sea benthic ecosystems. Elementa **5**: 4. doi:10.1525/elementa.203

Thiel, H., and G. Schriever. 1989. Cruise Report SO61. DISCOL 1. Balboa; 02.02.1989 – Callao: 03.04.1989. Zentrum für Meeres- und Klimaforschung der Universität Hamburg. Institut für Hydrobiologie und Fischereiwissenschaft.

Thiel, H., and F. Tiefsee-Umweltschutz. 2001. Evaluation of the environmental consequences of polymetallic nodule mining based on the results of the TUSCH Research Association. Deep-Sea Res. Part II **48**: 3433–3452. doi:10.1016/S0967-0645(01)00051-0

Thurber, A. R., A. K. Sweetman, B. E. Narayanaswamy, D. O. B. Jones, J. Ingels, and R. L. Hansman. 2014. Ecosystem function and services provided by the deep sea. Biogeosciences **11**: 3941–3963. doi:10.5194/bg-11-3941-2014

Vanreusel, A., A. Hilario, P. A. Ribeiro, L. Menot, and P. Martinez Arbizu. 2016. Threatened by mining, polymetallic noduels are required to preserve abyssal epifauna. Sci. Rep. **6**: 26808. doi:10.1038/srep26808

Wang, X., and W. E. Müller. 2009. Marine biominerals: Perspectives and challenges for polymetallic nodules and crusts. Trends Biotechnol. **27**: 375–383. doi:10.1016/j.tibtech.2009.03.004

Wiedicke, M. H., and E. M. Weber. 1996. Small-scale variability of seafloor features in the northern Peru Basin: Results from acoustic survey methods. Mar. Geophys. Res. **18**: 507–526. doi:10.1007/BF00310067

Yool, A., A. P. Martin, T. R. Anderson, B. J. Bett, D. O. Jones, and H. A. Ruhl. 2017. Big in the benthos: Future change of seafloor community biomass in a global, body size-resolved model. Glob. Chang. Biol. **23**: 3554–3566. doi: 10.1111/gcb.13680

Acknowledgments

The authors thank PI Antje Boetius, Felix Janssen, the scientific party, the captain and crew of RV *Sonne* as well as the ROV Kiel 6000 team from Geomar (Kiel) for their excellent support during cruise SO242-2. We thank the editor and two anonymous reviewers for their comments that helped to improve a previous version of this manuscript. The research leading to these results has received funding from the European Union Seventh Framework Programme (FP7/2007-2013) under the MIDAS project, grant agreement n° 603418 and by the JPI Oceans – Ecological Aspects of Deep Sea Mining project under NWO-ALW grant 856.14.002 and BMBF grant 03F0707A-G. AG in part was funded by the RSF grant 14-50-00095.

Conflict of Interest

None declared.

Submitted 12 June 2017
Revised 10 November 2017; 05 March 2018
Accepted 17 April 2018

Associate editor: Leila Hamdan

19395590, 2018, 5, Downloaded from https://aslopubs.onlinelibrary.wiley.com/doi/10.1002/lno.10929 by University Of Chemistry And, Wiley Online Library on [01/10/2026]. See the Terms and Conditions (https://onlinelibrary.wiley.com/terms-and-conditions) on Wiley Online Library for rules of use; OA articles are governed by the applicable Creative Commons License